ACS Medicinal Chemistry Letters
Cite This: ACS Med. Chem. Lett. 2019, 10, 1260−1265
Letter
pubs.acs.org/acsmedchemlett

Structure Based Design of Potent Selective Inhibitors of Protein Kinase D1 (PKD1)

Jianwen A. Feng,*[,†,⊥] Patrick Lee,[†] Moulay Hicham Alaoui,[†] Kathy Barrett,[†] Georgette Castanedo,[†] Robert Godemann,[§] Paul McEwan,[∥] Xiaolu Wang,[§] Ping Wu,[†] Yamin Zhang,[‡] Seth F. Harris,[†] and Steven T. Staben*[,†]

[†]Genentech, 1 DNA way, South San Francisco, California 94080, United States
[‡]Pharmaron Beijing Co., Ltd. 6 Taihe Road, BDA, Beijing, P.R. China, 100176
[§]Evotec AG, Manfred Eigen Campus, Essener Bogen, Hamburg, Germany 22419
[∥]Evotec (U.K.) Ltd, 114 Innovation Drive, Milton Park, Abingdon OX14 4Rz, U.K.

Supporting Information

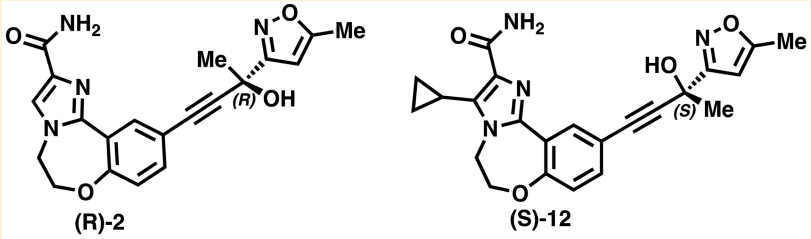

Compound	NIK ADP FP K_i (nM)	PKD1 ADP FP K_i (nM)	NIK ADP FP K_i/ PKD1 ADP FP K_i
(R)-2	3.1	4.9	0.6
(S)-12	1250	<0.2	>6250

ABSTRACT: We previously disclosed a series of type I 1/2 inhibitors of NF-κB inducing kinase (NIK). Inhibition of NIK by these compounds was found to be strongly dependent on the inclusion and absolute stereochemistry of a propargyl tertiary alcohol as it forms critical hydrogen bonds (H-bonds) with NIK. We report that inhibition of protein kinase D1 (PKD1) by this class of compounds is not dependent on H-bond interactions of this tertiary alcohol. This feature was leveraged in the design of highly selective inhibitors of PKD1 that no longer inhibit NIK. A structure-based hypothesis based on the position and flexibility of the α-C-helix of PKD1 vs NIK is presented.

KEYWORDS: *Structure-based drug design, kinase inhibitor, PKD1 (protein kinase D1), NIK (NF-κB inducing kinase)*

Selectivity remains a paramount challenge in the discovery and development of novel kinase inhibitors. In over 20 years of kinase-directed drug discovery, researchers have used numerous strategies to achieve sufficient selectivity for singular, or families of, kinases.[1,2] Among these strategies, differences in the so-called gatekeeper residue[3] are often exploited to achieve improved selectivity for active site inhibitors. Selectivity against off-target kinases with Phe or Tyr gatekeepers can be achieved by designing ligands that sterically clash with those larger residues. Polar or van der Waals contact with—and/or extension past—the gatekeeper residue by a ligand can provide enhanced selectivity in many cases.[4,5] The importance of the gatekeeper residue to kinase inhibitor binding is underscored in drug-induced resistance mutations (i.e., EGFR T90M post erlotinib treatment[6] or Abl T315I post imatinib treatment[7]).

Kinase inhibitors that bind to the DFG-in form, extend from the hinge past the gatekeeper residue, and interact with the DFG backbone and acidic α-C-helix residue are colloquially referred to as type I 1/2 kinase inhibitors (Figure 1a).[3,4] Zuccotto and Angiolini[3] postulate these hybrids of type I and II pharmacophores provide an opportunity to reach regions with differential plasticity and lower sequence conservation among kinases potentiating improved selectivity. The identification of inhibitors that fit the type I 1/2 pharmacophore is, however, dependent on the steric size of the gatekeeper residue.

We[4,5,8] and others,[9] have published type I 1/2 inhibitors of methionine gatekeeper kinases that include propargyl alcohol substitution. Exemplified by a ligand bound crystal structure of NIK (Figure 1b), an alkyne extends past the methionine gatekeeper and presents a tertiary alcohol to donate an H-bond to the conserved α-C-helix Glu and accept an H-bond from a backbone N−H from the DFG-motif Phe. Potent and selective inhibitors of several kinases including NIK,[4,8] AKT[10] (protein kinase B), and PAK4/5/6[5] have been achieved through

Received: December 31, 2018
Accepted: July 24, 2019
Published: July 24, 2019

DOI: 10.1021/acsmedchemlett.8b00658
ACS Med. Chem. Lett. 2019, 10, 1260−1265

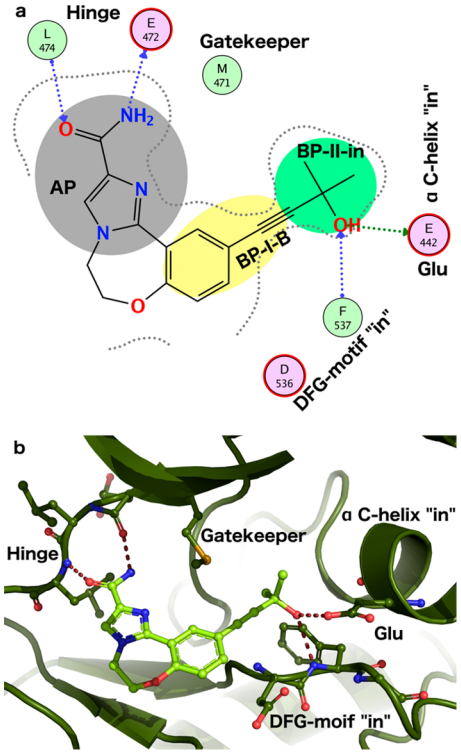

Figure 1. 2D and 3D representations of murine NIK with an inhibitor bound (PDB ID: 5T8O). (a) Schematic representation of an exemplar type I 1/2 kinase inhibitor. Gray dashed lines represent the ligand binding site. Green and blue arrows indicate ligand-protein hydrogen bonds. The inhibitor occupies the AP front subpocket, extends past the gatekeeper residue occupying the BP−I-B subpocket, and interacts with the acidic residue of the α-C-helix and a DFG-backbone N−H in the BP-II_in subpocket. Pocket nomenclature follows that of the KLIFS database.[2] (b) X-ray structure of murine NIK and a propargyl alcohol containing type I 1/2 inhibitor.[4]

utilization of this propargyl alcohol-driven pharmacophore. Herein we report that inhibition of PKD1 by this class of small molecules, in sharp contrast to other Met-gatekeeper kinases, does not require the tertiary alcohol. This somewhat unique characteristic was utilized in a structure-based design effort to discover highly selective inhibitors of PKD1.

We previously disclosed[4] several subseries of NIK inhibitors exemplified by compounds **1** and **2** (Table 1). We found the ability of these compounds to inhibit NIK was highly dependent on the stereochemistry of the propargylic alcohol. For example, the (R)-enantiomers of **1** and **2** maintained strong inhibition of NIK while the (S)-enantiomers lost >80-fold inhibitory potency. This stereodependent activity is readily rationalized through analysis of ligand soaked X-ray structures: key H-bond interactions of the tertiary alcohol and positioning of the heterocycle in the back pocket can only be accommodated by the (R)-enantiomer (*vide infra*). Of interest to the current study however, inhibitory activity against specific counter target PKD1 was not as strongly dependent on stereochemistry. For example, only an ∼3-fold loss in PKD1 potency was observed between (**R**)- and (**S**)-**2**.

This observation persisted with different propargyl alcohol substitution and was not specific to these subseries (select examples are shown in Table 2). Inhibitors bearing 2-methyl-5-oxazolyl substituted propargyl alcohols were found to be stronger inhibitors of PKD1 compared to NIK; the (S)-enantiomers demonstrating highest selectivity for PKD1 derived from steep loss of potency for NIK. Compound (**S**)-**3** was determined to have a NIK K_i > 1250 nM and a PKD1 K_i = 4.2 nM, a selectivity ratio of >298. Structurally distinct benzimidazole **4** displayed similar enantioselective behavior; (**R**)-**4** was very selective for NIK while (**S**)-**4** was moderately selective for PKD1. Comparing (**S**)-**3** with (**S**)-**4**, bridged bicycle series possessed a clear advantage over benzimidazoles in terms of selectivity for PKD1.

Introduction of a cyclopropyl group in the 3 position of the imidazole ring within this series further improves PKD1 inhibitory activity (Table 3). Compounds (**R**)-**5** and (**R**)-**6** were determined to have PKD1 K_i values of 5.9 nM and <0.2 nM, respectively. We hypothesize the >30-fold decrease in PKD1 K_i is a result of favorable van der Waals interactions with a leucine residue in the P-loop of PKD1 as the lipophilic ligand

Table 1. NIK and PKD1 Inhibition by Enantiomeric Pairs of Small Molecules

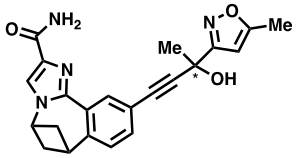

(R)-1, (S)-1

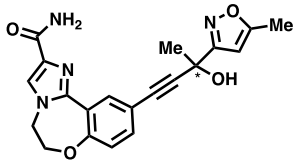

(R)-2, (S)-2

Compound	NIK ADP FP K_i(nM)[a]	PKD1 ADP FP K_i(nM)[a]	NIK ADP FP K_i/PKD1 ADP FP K_i
(**R**)-**1**	0.8	0.9	0.9
(**S**)-**1**	582	65	9
(**R**)-**2**	3.1	4.9	0.6
(**S**)-**2**	>250	14	>18

[a]See Supporting Information for assay experimental details

Table 2. NIK and PKD1 Inhibition by Small Molecules with Common 5-Methyloxazol-2-yl Propargyl Alcohol Substitution

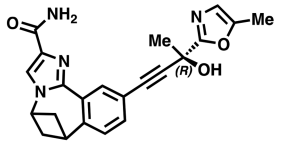

(R)-3

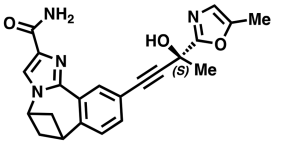

(S)-3

Compound	NIK ADP FP K_i(nM)[a]	PKD1 ADP FP K_i(nM)[a]	NIK ADP FP K_i/PKD1 ADP FP K_i
(**R**)-**3**	0.9	< 0.2	>4.5
(**S**)-**3**	>1250	4.2	>298

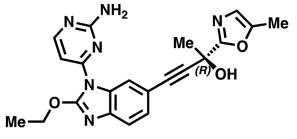

(R)-4

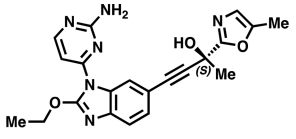

(S)-4

Compound	NIK ADP FP K_i(nM)[a]	PKD1 ADP FP K_i(nM)[a]	NIK ADP FP K_i/PKD1 ADP FP K_i
(**R**)-**4**	0.16	3.6	0.04
(**S**)-**4**	634	62	10.2

[a]See Supporting Information for assay experimental details.

DOI: 10.1021/acsmedchemlett.8b00658
ACS Med. Chem. Lett. 2019, 10, 1260−1265

Table 3. A Cyclopropyl Group Improves PKD1 Activity but Is Potency Neutral for NIK

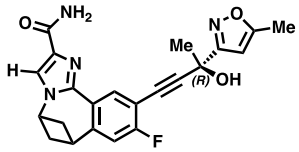

(R)-5

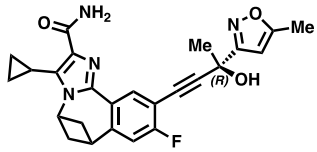

(R)-6

Compound	NIK ADP FP K_i(nM)[a]	PKD1 ADP FP K_i(nM)[a]	LogD$^{pH7.4}$	PKD1 LLE	NIK K_i/ PKD1 K_i
(R)-5	1.0	5.9	3.3	4.9	0.17
(R)-6	1.7	<0.2	3.7	>6.1	>8.5

[a]See Supporting Information for assay experimental details

efficiency (LLE)[11] for (R)-6 improved from 4.9 to >6.1(Figure 2). We believe that potency improvements were not observed

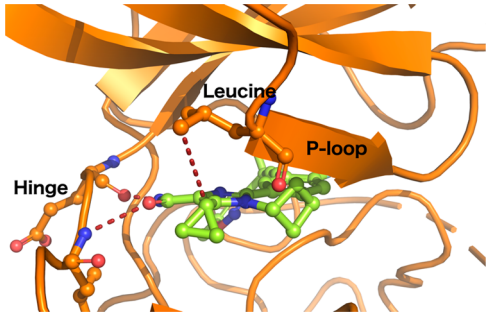

Figure 2. Model of (R)-6 bound to a homology model of PKD1 where a cyclopropyl group interacts with a leucine on the P-loop of PKD1. Corresponding leucine residue in NIK is flexible.

in NIK because the corresponding Leu406 residue is flexible and adopts multiple conformations as observed in human NIK crystal structures (4DN5, 4G3D, 4IDT, 4IDV).[12,8]

Compound (R)-7, a 14 nM NIK inhibitor, was soaked into murine NIK, and the X-ray structure was solved at 2.74 Å resolution (PDB ID: 6MYN). Modest ligand density was sufficient to describe the binding mode but did indicate partial ligand occupancy, refined to ~0.6 and 0.7 in the two copies present in the crystallographic asymmetric unit. The binding mode was as expected based on observations for similar compounds:[4] the primary amide interacting with the hinge residues Leu474 and Glu472, the alkyne projecting past the Met471 gatekeeper, the isoxazole occupying a hydrophobic pocket between the α-C-helix and gatekeeper, and the tertiary alcohol making the key donor/acceptor interactions consistent with type I1/2 description (Figure 3a). Of note is the position of the tertiary alcohol that is hypothesized to replace a key water observed in a 2.15 Å apo-structure (Figure 3b, apo structure in gray, PDB ID: 4G3C).[4,8,9] A model of the (S)-enantiomer indicates swapping of methyl and hydroxyl groups results in the inability of the ligand to form key hydrogen bonding interactions with NIK. We believe these results to be consistent with observed enantioselective NIK inhibition.

Based on the above models and enantiomer-dependent SAR for PKD1, we hypothesized ligands absent of the tertiary alcohol would inhibit PKD1 but not NIK. While 1-alkynyl-1-cyclopentanol **8** was similarly active against PKD1 and NIK, deletion of the hydroxyl as in 1-alkynylcyclopentane **9** resulted in a large loss in affinity for NIK (>125-fold) but not PKD1 (<2-fold) (Table 4). The drastic loss of potency against NIK

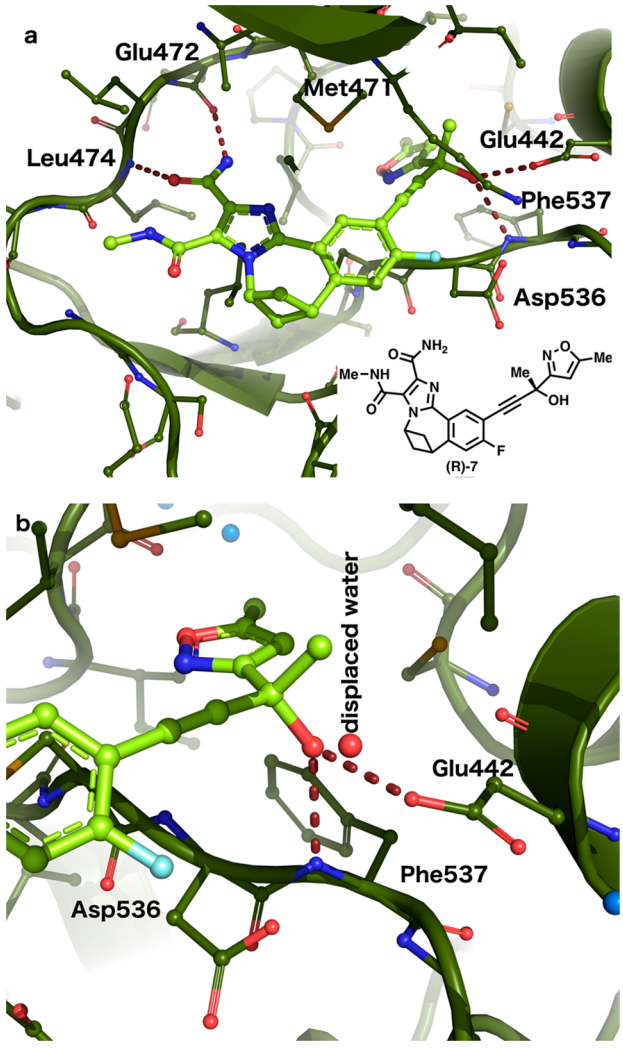

Figure 3. (a) X-ray structure of compound (R)-7 in mNIK (PDB ID: 6MYN). (b) Expanded image of (a) showing the interaction of the propargyl alcohol with Glu442 and Phe537. In the apo structure (PDB ID: 4G3C), Glu442 and Phe537 interact with a water molecule (labeled displaced water) that would be presumably displaced by compound (R)-7 and similar analogs. Model of the (S)-enantiomer swaps positions of methyl and hydroxyl groups resulting in the inability to maintain these hydrogen bonds.

Table 4. Influence of Hydroxyl Removal on Inhibition of NIK and PKD1

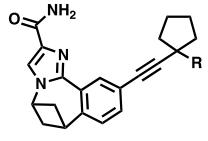

8, R = OH
9, R = H

Compound	NIK ADP FP K_i(nM)[a]	PKD1 ADP FP K_i(nM)[a]	NIK ADP FP K_i/ PKD1 ADP FP K_i
8 (R = OH)	10	25	0.4
9 (R = H)	>1250	44	>28

[a]See Supporting Information for assay experimental details.

for **9** is striking compared to **8** especially given the increased lipophilicity (cLogD$_{7.4}$ 4.0, 2.8, respectively): the LLE drops

DOI: 10.1021/acsmedchemlett.8b00658
ACS Med. Chem. Lett. 2019, 10, 1260−1265

from 5.2 to <1.9, pointing to the importance of mimicking a key water molecule with a hydroxyl function group for NIK.[8] Molecular modeling and SAR suggested that the hydroxyl could be directly replaced by a methyl group.

Analogs **10** and **11** combined 2-methyl-5-oxazolyl substitution and replaced the tertiary hydroxyl with a methyl group (Table 5). Introduction of a secondary amide group in compound **10** improved both NIK and PKD1 potency by forming an internal H-bond with the hinge binding amide (2.7 Å), potentially reducing electrostatic repulsion between primary amide carbonyl and protein backbone carbonyl (Figure 4a). Compounds **11** and **12** contain cyclopropyl imidazole substitutions to improve PKD1 activity. Achiral analogs **10** and **11** were among the most potent for PKD1 and highly selective over NIK (PKD1 K_i < 0.2 nM; NIK K_i > 1250 nM; > 6250-fold selective, Table 5). Replacing the tertiary hydroxyl group is critical for selectivity over NIK.

Table 5. Influence of Hydroxyl to Methyl Substitution and Imidazole Substitution on Inhibition of NIK and PKD1

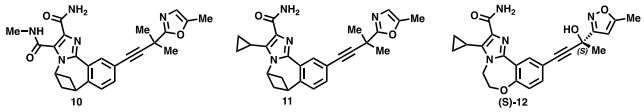

Compound	NIK ADP FP K_i(nM)[a]	PKD1 ADP FP K_i(nM)[a]	NIK ADP FP K_i/ PKD1 ADP FP K_i
10	>1250	<0.2	>6250
11	>1250	<0.2	>6250
(S)-12	>1250	<0.2	>6250

[a]See Supporting Information for assay experimental details

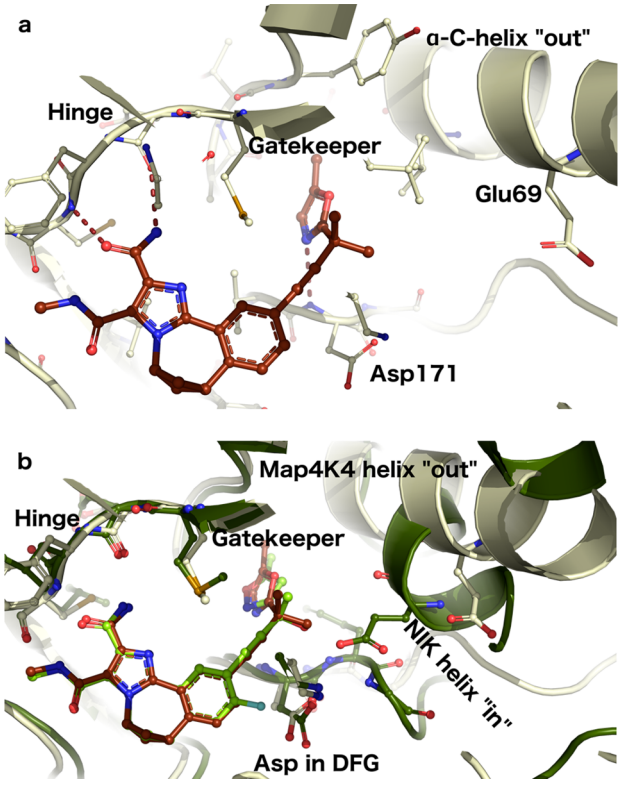

Figure 4. (a) X-ray structure of **10** bound to Map4K4 (PDB ID: 5W5Q). The primary amide in **10** forms expected H-bonding interactions with the Map4K4 kinase hinge. Gem-dimethyl groups cannot form H-bonds with the conserved Phe in DFG or Glu in α-C helix. (b) X-ray structure of compound **7** in mNIK (PDB ID: 6MYN) overlaid with compound **10** in Map4K4. Map4k4 adopts an α-C helix out conformation while NIK maintains an α-C helix in conformation.

Compound **(S)-12** was tested in a panel of kinases at Invitrogen at 0.1 μM, a concentration >500-fold its measured PKD1 K_i, and was found to be highly selective for PKD1. Among the 220 kinases tested, only PKD1 was inhibited at >30% (see Supporting Information for details). Included in this panel were a number of kinases bearing a methionine gatekeeper, none of which were strongly inhibited (i.e., AKT1, 4% inhibition; JAK1, 1%; Map4K4, 21%; Mink1, 20%; PAK4, 7%). Selectivity over NIK can be attributed to S stereochemistry of the tertiary alcohol as it is geometrically prevented from forming hydrogen bonds with Glu442 and Phe537. Compound **11** had equally exquisite kinase selectivity where Aurora B was the only off-target inhibited at greater than 40%. Compound **10** was also very selective when tested in the same panel at 0.1 μM concentration, most notably inhibiting Map4K4 (57%), Mink1 (51%), and Aurora B (45%) in addition to PKD1.

We sought to understand the molecular basis of the PKD1 versus NIK selectivity for ligands such as **10**–**12**. An X-ray structure of PKD1 has not been published. However, compound **10** possesses some affinity for Map4K4 (57% inhibition at 0.1 μM) and, having similarity in a longer β3-αC helix loop length (*vide infra*), we believed a Map4K4 structure might provide improved understanding of potential binding modes of these compounds in PKD1.[13] An X-ray structure of **10** (2.3 Å resolution, PDB ID: 5W5Q) is displayed in Figure 4a. As expected, the amide group forms two H-bond interactions with Map4K4's kinase hinge residues. The alkynyl linker projects an oxazole group that occupies a hydrophobic pocket partly formed by the gatekeeper methionine. Unlike propargyl alcohol-containing NIK inhibitors, compound **10** lacks a hydroxyl group that can form hydrogen bonds with the conserved Phe backbone NH or α-C helix Glu.[4] In fact, the MAP4K4 α-C helix is in the kinase inactive "out" position, further supporting our hypothesis that PKD1 inhibitors do not need a H-bonding hydroxyl group to achieve high affinity. Figure 4b shows an overlay of compound **7** bound to NIK (green) and compound **10** bound to Map4K4 (brown). Near perfect overlay of compounds **7** and **10** in the respective NIK and Map4K4 structures indicates consistent binding modes relative to the kinase hinge and general ATP pocket. A striking difference is observed, however, in the outward shift of Map4K4's α-C helix that explains compound **10**'s selectivity profile. The length of the β3-αC loop that precedes the α-C helix has been observed to affect α-C helix position and mobility, and hence kinase activity and sensitivity to certain classes of inhibitors.[14] Longer loops, as measured by the number of residues between the conserved catalytic lysine and the acidic Glu on helix C (e.g., 16, 17, or 14 as observed in EGFR, RAF, or SrcA/B family kinases, respectively), allow outward helix C positions and accommodate larger type II kinase inhibitors, while deletions of ~5 residues in these loops favor α-C helix "in" conformations making the mutant kinases more active and resistant to the larger inhibitors. The NIK α-C helix is constrained by both a short β3–αC loop (11 residues) and the presence of an unusual additional amino terminal helix that packs against and stabilizes the α-C helix-"in" feature. Consistent with shorter loop examples,[14] NIK is a constitutively active kinase and has reduced affinity for

DOI: 10.1021/acsmedchemlett.8b00658
ACS Med. Chem. Lett. 2019, 10, 1260–1265

compounds such as **10** that fit poorly in α-C helix in conformations. Map4K4 and PKD1 meanwhile have longer β3−αC loops (15 and 18 residues, respectively). We hypothesize the longer loop imparts less energetic barrier to helix C out conformations and is reflected in better binding affinity for compound **10**.

Compounds **10**−**12** are exquisitely selective and highly potent PKD1 inhibitors, making them potentially valuable tool compounds to interrogate PKD1 biology in immunology, oncology, and cardiology.[15−17] They also have reasonable *in vitro* ADME properties (Table 6). For example, compound **(S)-12** is predicted to have moderate *in vivo* clearance given its low measured logD and moderate liver microsomal clearance in human and rat.

Table 6. *In Vitro* ADME Properties of PKD1 Inhibitors

	LogD pH7.4	Kinetic Solubility	LM stability (mL/min/kg) H/R/M	Permeability A to B/B to A
10	3.7	13 μM	18/26/74	19.3/14.9
11	4.4	35 μM	19/45/84	13.8/14.1
(S)-12	2.0	124 μM	9.5/35/78	7.1/16.0

In conclusion, we discovered a series of highly selective PKD1 inhibitors that exhibit subnanomolar biochemical potency. These pseudo type I1/2 inhibitors derive their selectivity by extending past the methionine gatekeeper and favoring kinases that can adopt α-C-helix "out" conformations. Type I1/2 kinase inhibitors interact with a conserved α-C-helix glutamate residue, therefore requiring the helix C "in" conformation. The crystal structure of compound **10** bound to surrogate kinase Map4K4 shows it adopting a helix C "out" conformation. The novel combination of extending past the gatekeeper residue and requiring helix C "out" conformation provides structural rationale for the observed exquisite selectivity of compounds **10**−**12**. Given successful generation of selective inhibitors of several methionine gatekeeper kinases (PKD1, NIK, AKT, PAKs) utilizing an alkyne-driven binding mode, we believe this could be a generalizable strategy for generating tool compounds of methionine gatekeeper kinases.

■ ASSOCIATED CONTENT

Supporting Information

The Supporting Information is available free of charge on the ACS Publications website at DOI: 10.1021/acsmedchemlett.8b00658.

Details of PKD1 enzyme inhibition assay, crystallography, kinase selectivity for compounds **10**, **11**, and (S)-**12**, synthetic procedures, and analytical data (PDF)

■ AUTHOR INFORMATION

Corresponding Authors

*Jianwen A. Feng, jw.a.feng@gmail.com.
*Steven T. Staben, stevents@gene.com.

ORCID

Jianwen A. Feng: 0000-0003-1221-7605
Steven T. Staben: 0000-0002-6137-6517

Present Address

[⊥]Denali Therapeutics Inc., 161 Oyster Point Blvd, South San Francisco, CA 94080.

Author Contributions

The manuscript was written through contributions of all authors. All authors have given approval to the final version of the manuscript.

Notes

The authors declare the following competing financial interest(s): JAF is an employee and stockholder for Denali. MHA, KB, NB, GC, PW, SFH, and STS are employees and stockholders for Roche.

■ ACKNOWLEDGMENTS

We thank the Genentech purification and analytical groups for support. We acknowledge the use of synchrotron X-ray source SSRL supported by the Department of Energy's (DOE) Office of Science, Office of Biological and Environmental Research, and the National Institutes of Health (NIH). The authors thank the staff at Diamond Light Source beamline I04-1 and Stanford Synchrotron Radiation Light Source beamline 12-2.

■ ABBREVIATIONS

PKD1,protein kinase D1; AKT,protein kinase B; PAK,p21-activated kinase; NIK,NF-κB inducing kinase; LLE,ligand lipophilic efficiency (pIC50 − LogD).

■ REFERENCES

(1) Davis, M. I.; Hunt, J. P.; Herrgard, S.; Ciceri, P.; Wodicka, L. M.; Pallares, G.; Hocker, M.; Treiber, D. K.; Zarrinkar, P. P. Comprehensive Analysis of Kinase Inhibitor Selectivity. *Nat. Biotechnol.* **2011**, *29* (11), 1046−1051.

(2) van Linden, O. P. J.; Kooistra, A. J.; Leurs, R.; de Esch, I. J. P.; de Graaf, C. KLIFS: a Knowledge-Based Structural Database to Navigate Kinase−Ligand Interaction Space. *J. Med. Chem.* **2014**, *57* (2), 249−277.

(3) Zuccotto, F.; Ardini, E.; Casale, E.; Angiolini, M. Through the "Gatekeeper Door": Exploiting the Active Kinase Conformation. *J. Med. Chem.* **2010**, *53* (7), 2681−2694.

(4) Castanedo, G. M.; Blaquiere, N.; Beresini, M.; Bravo, B.; Brightbill, H.; Chen, J.; Cui, H.-F.; Eigenbrot, C.; Everett, C.; Feng, J.; Godemann, R.; Gogol, E.; Hymowitz, S.; Johnson, A.; Kayagaki, N.; Kohli, P. B.; Knüppel, K.; Kraemer, J.; Krüger, S.; Loke, P.; McEwan, P.; Montalbetti, C.; Roberts, D. A.; Smith, M.; Steinbacher, S.; Sujatha-Bhaskar, S.; Takahashi, R.; Wang, X.; Wu, L. C.; Zhang, Y.; Staben, S. T. Structure-Based Design of Tricyclic NF-κB Inducing Kinase (NIK) Inhibitors That Have High Selectivity Over Phosphoinositide-3-Kinase (PI3K). *J. Med. Chem.* **2017**, *60* (2), 627−640.

(5) Staben, S. T.; Feng, J. A.; Lyle, K.; Belvin, M.; Boggs, J.; Burch, J. D.; Chua, C.-C.; Cui, H.; DiPasquale, A. G.; Friedman, L. S.; Heise, C.; Koeppen, H.; Kotey, A.; Mintzer, R.; Oh, A.; Roberts, D. A.; Rouge, L.; Rudolph, J.; Tam, C.; Wang, W.; Xiao, Y.; Young, A.; Zhang, Y.; Hoeflich, K. P. Back Pocket Flexibility Provides Group II P21-Activated Kinase (PAK) Selectivity for Type I 1/2 Kinase Inhibitors. *J. Med. Chem.* **2014**, *57* (3), 1033−1045.

(6) Bell, D. W.; Gore, I.; Okimoto, R. A.; Godin-Heymann, N.; Sordella, R.; Mulloy, R.; Sharma, S. V.; Brannigan, B. W.; Mohapatra, G.; Settleman, J.; Haber, D. A. Inherited Susceptibility to Lung Cancer May Be Associated with the T790M Drug Resistance Mutation in EGFR. *Nat. Genet.* **2005**, *37* (12), 1315−1316.

(7) Shah, N. P.; Tran, C.; Lee, F. Y.; Chen, P.; Norris, D.; Sawyers, C. L. Overriding Imatinib Resistance with a Novel ABL Kinase Inhibitor. *Science* **2004**, *305* (5682), 399−401.

(8) de Leon-Boenig, G.; Bowman, K. K.; Feng, J. A.; Crawford, T.; Everett, C.; Franke, Y.; Oh, A.; Stanley, M.; Staben, S. T.; Starovasnik, M. A.; Wallweber, H. J. A.; Wu, J.; Wu, L. C.; Johnson, A. R.; Hymowitz, S. G. The Crystal Structure of the Catalytic Domain of the

DOI: 10.1021/acsmedchemlett.8b00658
ACS Med. Chem. Lett. 2019, 10, 1260−1265

NF-KB Inducing Kinase Reveals a Narrow but Flexible Active Site. *Structure* **2012**, *20* (10), 1704−1714.
(9) Li, K.; McGee, L. R.; Fisher, B.; Sudom, A.; Liu, J.; Rubenstein, S. M.; Anwer, M. K.; Cushing, T. D.; Shin, Y.; Ayres, M.; Lee, F.; Eksterowicz, J.; Faulder, P.; Waszkowycz, B.; Plotnikova, O.; Farrelly, E.; Xiao, S.-H.; Chen, G.; Wang, Z. Inhibiting NF-κB-Inducing Kinase (NIK): Discovery, Structure-Based Design, Synthesis, Structure−Activity Relationship, and Co-Crystal Structures. *Bioorg. Med. Chem. Lett.* **2013**, *23* (5), 1238−1244.
(10) Rouse, M. B.; Seefeld, M. A.; Leber, J. D.; McNulty, K. C.; Sun, L.; Miller, W. H.; Zhang, S.; Minthorn, E. A.; Concha, N. O.; Choudhry, A. E.; Schaber, M. D.; Heerding, D. A. Aminofurazans as Potent Inhibitors of AKT Kinase. *Bioorg. Med. Chem. Lett.* **2009**, *19* (5), 1508−1511.
(11) Leeson, P. D.; Springthorpe, B. The Influence of Drug-Like Concepts on Decision-Making in Medicinal Chemistry. *Nat. Rev. Drug Discovery* **2007**, *6* (11), 881−890.
(12) Liu, J.; Sudom, A.; Min, X.; Cao, Z.; Gao, X.; Ayres, M.; Lee, F.; Cao, P.; Johnstone, S.; Plotnikova, O.; Walker, N.; Chen, G.; Wang, Z. Structure of the Nuclear Factor B-Inducing Kinase (NIK) Kinase Domain Reveals a Constitutively Active Conformation. *J. Biol. Chem.* **2012**, *287* (33), 27326−27334.
(13) Crawford, T. D.; Ndubaku, C. O.; Chen, H.; Boggs, J. W.; Bravo, B. J.; DeLaTorre, K.; Giannetti, A. M.; Gould, S. E.; Harris, S. F.; Magnuson, S. R.; McNamara, E.; Murray, L. J.; Nonomiya, J.; Sambrone, A.; Schmidt, S.; Smyczek, T.; Stanley, M.; Vitorino, P.; Wang, L.; West, K.; Wu, P.; Ye, W. Discovery of Selective 4-Amino-Pyridopyrimidine Inhibitors of MAP4K4 Using Fragment-Based Lead Identification and Optimization. *J. Med. Chem.* **2014**, *57* (8), 3484−3493.
(14) Foster, S. A.; Whalen, D. M.; Özen, A.; Wongchenko, M. J.; Yin, J.; Yen, I.; Schaefer, G.; Mayfield, J. D.; Chmielecki, J.; Stephens, P. J.; Albacker, L. A.; Yan, Y.; Song, K.; Hatzivassiliou, G.; Eigenbrot, C.; Yu, C.; Shaw, A. S.; Manning, G.; Skelton, N. J.; Hymowitz, S. G.; Malek, S. Activation Mechanism of Oncogenic Deletion Mutations in BRAF, EGFR, and HER2. *Cancer Cell* **2016**, *29* (4), 477−493.
(15) Sundram, V.; Chauhan, S. C.; Jaggi, M. Emerging Roles of Protein Kinase D1 in Cancer. *Mol. Cancer Res.* **2011**, *9* (8), 985−996.
(16) Meredith, E. L.; Beattie, K.; Burgis, R.; Capparelli, M.; Chapo, J.; DiPietro, L.; Gamber, G.; Enyedy, I.; Hood, D. B.; Hosagrahara, V.; Jewell, C.; Koch, K. A.; Lee, W.; Lemon, D. D.; McKinsey, T. A.; Miranda, K.; Pagratis, N.; Phan, D.; Plato, C.; Rao, C.; Rozhitskaya, O.; Soldermann, N.; Springer, C.; van Eis, M.; Vega, R. B.; Yan, W.; Zhu, Q.; Monovich, L. G. Identification of Potent and Selective Amidobipyridyl Inhibitors of Protein Kinase D. *J. Med. Chem.* **2010**, *53* (15), 5422−5438.
(17) Hao, Q.; Wang, L.; Tang, H. Vascular Endothelial Growth Factor Induces Protein Kinase D-Dependent Production of Proinflammatory Cytokines in Endothelial Cells. *AJP: Cell Physiology* **2009**, *296* (4), C821−C827.

DOI: 10.1021/acsmedchemlett.8b00658
ACS Med. Chem. Lett. 2019, 10, 1260−1265